Prediction of neutron source, tritium production and activation for long-pulse operation of the ITER Neutral Beam Test Facility

S J Cox, A Emmanoulidis, T T C Jones and M J Loughlin

EURATOM/UKAEA Fusion Association, Culham Science Centre, Abingdon, Oxfordshire, OX14 3DB, United Kingdom. Email: timothy.jones@jet.uk

Abstract

A Local Mixing Model (LMM)[1] has been utilised to compute the evolution of the hydrogen isotope content within the implantation zone of the CuCrZr target material of the beam-stopping elements of the ITER Neutral Beam Test Facility, together with the beam-target fusion reaction rate calculated by taking account of the slowing-down of the 1MeV incoming projectile ion within the implantation layer. An important modification of the LMM code is to treat the tritium reaction product ions, resulting from D-D reactions, as a constituent of the incident beam. Although the treatment of tritium in the LMM is not ideal, this and other simplifying assumptions either do not significantly affect the predictions, or ensure conservatism in the results when used as input to the safety analysis of the facility. For example, it is shown that T→D "beam-target" reactions always dominate over those of D→T, which overcomes the problem of uncertainty, in the model, of the distribution of tritium trapped within the implantation layer; in contrast there is little uncertainty that this region will rapidly approach deuterium saturation for long-pulse (≤ 1hr) operation. Using the computed sources as input, neutronics and activation calculations for the NBTF components have been carried out using the MCNP/FISPACT. As expected, long-pulse operational requirements lead to neutron activation and tritium production levels which have non-negligible but manageable radiological consequences.

This work was conducted under the European Fusion Development Agreement and funded by Euratom and the UK Engineering and Physical Science Research Council.

[1] H-D Falter *et al*, Proc. 17th Symposium on Fusion Technology, Rome (1992) p 481

1. Introduction

As part of the safety analysis of the Neutral Beam Test Facility (NBTF) foreseen for ITER, a quantitative assessment of neutron production, component activation and tritium formation/accumulation is necessary. These key radiological factors determine the radiation shielding parameters, the hands-on maintainability of beamline components, and dictate the requirements for eventual licensing of the facility. Since a possible approach to the NBTF is to consider the beamline and ancillary equipment as parts of the first ITER injector, it is also important to be able to assess the transportability of the main components. The ITER neutral beam injector will accelerate deuterons to 1MeV. During operation of the NBTF the deuterons will be dumped onto a residual ion dump and calorimeter which will therefore become loaded with deuterium. Further incoming beam particles may undergo the reactions $d(d,n)^3He$ and $d(d,p)^3H$. The neutrons are emitted with an energy of approximately 2.5MeV. This reaction is the most important mechanism of neutron production from the NBTF. The production of tritium (^3H), in the second branch of the DD reaction, is itself a radiological concern but it also implies the further production of 14MeV neutrons by the tritons reacting with the deuterium in the calorimeter or with incoming beam deuterons. Neutron production leads to a potential radiation exposure to workers either directly, during beam operation, or as a result of neutron activation of the injector and the subsequent γ-ray emission. It is important to quantify these radiological aspects in order to define an operational plan such that excessive activation of the injector is avoided and that there are no difficulties in maintaining or subsequently transporting and deploying the injector at ITER. Calculations of neutron production rates and deuterium and tritium accumulation in the target material have been performed using a Local Mixing Model (LMM) calculation code [1,2,3]. The LMM has been modified in the present work to take into account tritium produced by the DD reactions. The modified version of the code can therefore calculate both 2.5 MeV (DD) and 14 MeV (DT and TD) neutron rates which represent the basic source terms for the radiological safety analysis. The LMM and its adaptation to compute the rate of secondary (DT) reactions are described in Section 2; the limitations of the model are discussed in Section 3 but it is shown that such limitations either do not affect the results or would lead to conservatism in the safety analysis. The issue of tritium inventory build-up in the NBTF is discussed in Section 4. The neutron transport and activation were calculated using the Monte-Carlo code MCNP [4] version 4c3 and the inventory code FISPACT [5] using the neutron production estimates from the LMM. The results of the activation analysis are briefly summarised in Section 5.

2. Local Mixing Model

The Local Mixing Model in its standard form assumes that the beam particles are incident normal to the surface of a target and slow down inside the material to be trapped when they come to rest. The density of implanted ions increases until a saturation density is reached, after which the particles of the beam start displacing already trapped ions with a release rate equal to the deposition rate. The composition of the released ions reflects the implanted species mixture in the trap. In the case of two different species (denoted by suffix 1, 2) the differential equations for the rate of change of local density are:

$$(1)\begin{cases}\dfrac{dn_1(x)}{dt} = p_1(E_1, x)\cdot\Phi_1 \\ \dfrac{dn_2(x)}{dt} = p_2(E_2, x)\cdot\Phi_2\end{cases}$$

(locally non saturated target: $n_1+n_2<n_{sat}$),

$$(2)\begin{cases}\dfrac{dn_1(x)}{dt} = \dfrac{n_2(x)}{n_{sat}}\cdot p_1(E_1, x)\cdot\Phi_1 - \dfrac{n_1(x)}{n_{sat}}\cdot p_2(E_2, x)\cdot\Phi_2 \\ \dfrac{dn_2(x)}{dt} = -\dfrac{dn_1(x)}{dt}\end{cases}$$

(locally saturated target: $n_1+n_2=n_{sat}$),

where $n_i(x)$ is the density of trapped ions, Φ_i is the flux of incoming particles and $p_i(E_i, x)dx$ is the probability for particle i with energy E_i to come to rest in the range $(x, x+dx)$.

The LMM code calculates the function $p(E, x)$ for each component (H, D and T) of the incoming beam, then solves iteratively the above differential equations to calculate the distribution profile matrices at each iteration for the three isotopes. The LMM code also contains a slowing-down routine for each incoming projectile species, based on the energy-dependent stopping-power of the ions. The results of the slowing-down calculation are folded in with the relevant fusion reaction cross-section to compute the reaction rate at each iteration. The iterations stop when the required total time of integration is achieved.

2.1 Benchmarking of LMM

The LMM code has been applied previously to model isotopic exchange in the JET Neutral Beam Test Bed [2,3], for positive-ion beams of energy 80-140keV. In these experiments, the 2.5MeV neutron production from the ion dumps was measured after changing the beam gas from hydrogen to deuterium. In this situation, the target material is initially saturated with hydrogen which is progressively replaced by deuterium, and indicated by the evolution of the neutron rate. Good agreement between the predicted and measured neutrons was obtained if the saturation density of the implanted hydrogenic species was taken to be about 10% of the Cu atom density of the material, which may be compared with a typical maximum saturation density of about 20% at room temperature. This is reasonable since the surface temperature T of the ion dump high heat-flux elements can reach >400^{o}C, and the hydrogen saturation density is expected to vary as 1/T. Other authors (e.g. [6]) have also reported evidence of reduced saturation densities to explain the observed beam-target reaction rates in NB injectors. In order to benchmark the cross-section and energy-loss tables embedded in the LMM code in the present work, the predictions of the LMM for D beams impinging on a Cu target were compared with the analytic model of Kim [7,8] at incident particle energies up to 1MeV at the same target saturation density. The LMM code with a saturated target (20% of Cu atom density), and a deuterium beam of 1 MeV and current density of 1 mA/cm^2, gives a constant flux of 3.78×10^{12} neutrons per cm^2 per C of incoming deuterium beam, in agreement with Kim's formula within 7%. We can therefore conclude that the LMM output is in good agreement with the benchmark for the calculation of the neutron rate of a 1 MeV deuterium beam on a copper surface.

2.2 Application of LMM to ITER NBTF operation

A reference NBTF pulse of 1 hour duration, with a beam of 1 MeV deuterium and total current of 40 A, with a maximum target current density of 1 mA cm^{-2} is assumed [9]. The total working life of the injector is expected to be around 250 hours; including a final reliability run of 84 hours spread over two weeks and three reference campaigns of 100 days duration, assuming 100 pulses of 20 seconds per day at full power (55.5 hours per campaign). Starting with a fully depleted target, ions of the incoming deuterium beam fill the material until the saturation concentration (20%) is reached. Although a saturation density of less than 20% has been suggested as being more representative [6], a pessimistic assumption is to use

20%. The most probable implantation depth for 1MeV D^+ is about 5.5 μm. The total retained deuterium increases as the implanted ions fill regions closer to the surface and deeper inside the material. By integrating the implantation density profile with respect to depth, the areal density of the implanted species is obtained as a function of the number of beam pulses (pulse length of 3600 s and a beam of 1 MeV, 1 mA cm^{-2} of D^+); 80% of the maximum areal implantation density is reached in around 60 1-hour pulses at this current density. In view of the relatively fast approach to saturation, the simplifying assumption of a fully deuterium-saturated target to a depth of 10 μm is made for all calculations presented in the rest of the paper, corresponding to an implanted deuterium areal density of $1.7\times10^{19}cm^{-2}$. Under this assumption, the DD reaction rate per unit area is linear with beam current density and independent of integrated beam fluence, according to the constant ratio of 3.78×10^{12} neutrons per incident Coulomb of beam deuterons. It is worth noting that the total number of DD neutrons produced in one 1-hour duration 40 A pulse, is therefore predicted to be $5.4\cdot10^{17}$ neutrons. This is comparable with a high power JET deuterium plasma pulse, albeit on a much longer time-scale.

2.3 Treatment of secondary DT reactions in the LMM

The nuclear reactions in the metal target due to the interaction of the incoming deuterium beam and the deuterium already trapped in the target are:

$$\begin{cases} D + D \xrightarrow[50\%]{} \mathrm{He}^3 + \mathrm{n} & Q = 3.27\mathrm{MeV} \\ D + D \xrightarrow[50\%]{} \mathrm{T} + \mathrm{p} & Q = 4.03\mathrm{MeV} \end{cases}$$

The total energy of the reaction products must be the sum of the reaction Q-value (4.033 MeV) and the beam energy (≤ 1 MeV for the ITER NB accelerator). The way in which this total energy is shared between the fragments is dictated by the angle between the velocity of the fragments and the incoming D, according to the conservation of the total momentum. The probability of the fragment to be generated with a given angle is not constant, because an angular probability distribution characterises each nuclear reaction. From the knowledge of the angular distribution of the energies of the T (Figure 1) and the probability of each angle, it is possible to calculate the probability distribution of the T energy, as shown in Figure 2. It is interesting to note that the most probable energies for the triton lie in the range 0.9 to 1.3

MeV (corresponding to an angle of 60-80 degrees between the incoming D and the generated T). The fact that the most probable energy of the triton is very close to the energy of the deuterium beam suggests the possibility of treating the tritons produced inside the target as part of the incoming beam in a modified version of the LMM code. The modified LMM code, at each iteration, calculates the equivalent tritium beam produced by the DD reactions, adds this tritium to the incoming deuterium beam and runs the iteration as normal, but with a composite D-T beam, by iteratively solving equations (1) and (2). This approximation was considered the simplest to implement in the existing code, though it has a number of limitations as discussed in Section 3.

2.4 DT reactions and 14MeV neutron production rates

In the treatment of tritium production and secondary DT reactions according the simplifying assumptions described in the previous paragraph, reactions take place between (a) fast T^+ and the implanted D atoms in the saturation zone (denoted T→D) and (b) fast D^+ and implanted T atoms (denoted D→T). Since the T^+ is treated as a component of the incoming beam, the capability of the LMM code to calculate the evolution of the isotopic composition of the implanted hydrogenic atoms, according to the solution of equations (1) and (2) for a 2-component system, is exploited. The D→T contribution to the reaction rate depends on the tritium concentration which slowly builds up with time within the implantation layer, according to the deuterium beam fluence (Table 1).

Pulses	Fluence D [C cm^{-2}]	Fluence T [C cm^{-2}]	DT neutr. [C^{-1} cm^{-2}]	TD neutr. [C^{-1} cm^{-2}]	Ret. T [cm^{-2}]
500	$1.8\cdot10^{3}$	$1.09\cdot10^{-3}$	$1.2\cdot10^{5}$	$5.2\cdot10^{7}$	$1.0\cdot10^{10}$
5000	$1.8\cdot10^{4}$	$1.09\cdot10^{-2}$	$1.5\cdot10^{5}$	$5.2\cdot10^{7}$	$1.5\cdot10^{10}$
50000	$1.8\cdot10^{5}$	$1.09\cdot10^{-1}$	$1.9\cdot10^{5}$	$5.2\cdot10^{7}$	$2.2\cdot10^{10}$

Table 1: D→T and T→D reaction rates and T retention within implantation zone for the number of 1-hour pulses shown

The T→D reaction rate per unit area is linear with D^+ current density and independent of beam fluence. This is because the tritium concentration is only $\approx10^{-9}$ that of deuterium and so the deuterium target remains almost constant.

3. **Limitations of Local Mixing Model applied to NBTF**

A number of simplifying assumptions have been made in the application of the LMM as described in the previous section. For the purposes of the present work, it is important to ensure that the source rates of neutrons and tritium are conservative i.e. represent upper limits. In this section it is shown that the simplifying assumptions satisfy this requirement, or alternatively have no significant influence on the results.

3.1 Effect of non-normal beam incidence

The LMM model assumes a normal angle of incidence for the incoming beam particles. In reality, the angle of incidence tends to be much lower as the beam stopping elements may be inclined to the beam in order to reduce the power and current density [9]. This reduces the mean penetration depth of the beam particles, measured normal to the surface, by a factor $\sin\theta$ where θ is the angle of the beam with respect to the surface, and implies that the filling of the target will be more rapid as the angle of incidence is reduced (at constant current density normal to the surface). This strengthens the assumption made in Section 2.2 that the incoming fast ions slow down within a region that is fully saturated, and therefore the effect of non-normal angle of incidence does not change the calculations of neutron and tritium source rates. It should be noted that the angle of incidence between the beam and the target must be taken into account when determining the magnitude of the current density normal to the surface, as input to the calculation of the local source rates on particular beam-stopping elements. Normal incidence is assumed for all calculations using the LMM.

3.2 Retained tritium density distribution in the implantation zone

The modelling of tritium as a beam in the modified LMM code is not optimal and does not treat correctly the localisation of the fast tritium source or its velocity distribution. The incoming deuterons give up a large fraction of their kinetic energy in a small volume at the end of their range, the so called Bragg ionisation peak. A consequence of this is that the tritons are most likely to be born around the mean penetration depth, R_D, of the deuterium (~5.6 μm from the surface, as shown in Figure 3). The actual distribution of implanted tritium will be broader and more uniform than that computed on the basis of a monoenergetic

incident beam at the material surface. Since some tritons are generated with the same velocity direction as the incoming D beam, they will travel deeper into the material, coming to rest beyond the maximum deuterium penetration depth and hence will not be accessible by incoming D for subsequent D→T reactions. Furthermore, tritons are generated with an energy of up to 2.8 MeV (Figure 1), much larger than the 1 MeV assumed by the model, allowing them to travel even deeper. A different approach to the problem consists of redistributing uniformly the tritons inside the target (up to a depth of 10 μm) after each step. This depth corresponds approximately to the sum of the penetration depths R_D and R_T of 1MeV D and and 1MeV T respectively. Results of the comparison of the two approaches for 500 1-hour beam pulses are shown in Table 2.

	T fluence [cm^{-2}]	**DT neutr. [C^{-1} cm^{-2}]**	**TD neutr. [C^{-1} cm^{-2}]**
Non Redistributed T	$6.8 \cdot 10^{15}$	$1.2 \cdot 10^{5}$	$5.2 \cdot 10^{7}$
Redistributed T	$6.8 \cdot 10^{15}$	$6.0 \cdot 10^{4}$	$5.2 \cdot 10^{7}$

Table 2: Comparison of results with and without T redistribution within the deuterium implantation zone

The redistribution process halves the rate of D→T neutrons. This is due to the relocation of many tritons deeper into the material in the region not reached by the incoming deuterons (with a maximum penetration depth of less than 6 μm in copper). No difference is evident for T→D neutrons as expected. We can therefore conclude that the non-redistribution case is the most pessimistic evaluation of the neutron production rate; in any case the upper limit of the D→T contribution (which is the least well modelled component) is <1% of the total DT reaction rate and can be neglected in practice.

4. **Tritium build-up and removal**

4.1 Combined isotopic exchange and thermal diffusion model

The isotopic exchange model built into the LMM only treats the zone which is accessed, by implantation, of both species (D and T), since the LMM exchange mechanism is displacement of one trapped atom by one incoming atom at the point where the latter comes to rest. Therefore, the areal tritium concentrations predicted by the LMM (Table 1), amounting to an extremely small proportion of the total tritium production, do not include

tritium that penetrates beyond the deuterium implantation zone i.e. in the range of R where $R_D<R<R_D+R_T$, as discussed in Section 3.2. One of the aims of the safety analysis of the NBTF is to quantify the long-term tritium retention of the beamline components, for which the LMM isotopic exchange model alone is inadequate. This statement follows from the fact that the results must include a margin of conservatism, and the LMM predictions of the retained tritium are evidently an underestimate. The evolution of the tritium density beyond the deuterium implantation zone is governed by thermal diffusion processes. The transport of tritium can therefore be described in three distinct zones as follows.

Zone (1), $0<R<R_D$:	isotopic exchange with incoming D;
Zone (2), $R_D<R<R_D+R_T$:	thermal diffusion towards the surface;
Zone (3), $R_D+R_T<R<L$	thermal diffusion into the bulk, eventually reaching the water cooling channel located at R=L=2mm.

In Zone (1) it is reasonable to take the average T density n_0 from the LMM (non redistribution case, Section 3.2) as an upper limit in order to define a boundary condition at $R=R_D$. From Table 1, after 500 hours operation at a D beam current density of $1mAcm^{-2}$ the corresponding value of $n_0 = (1\times10^{10}cm^{-2}/R_D) = (1\times10^{10}cm^{-2}/5.6\times10^{-4}cm) = 1.79\times10^{13}cm^{-3}$. The diffusive flow in zones (2) and (3) is balanced by the tritium source due to deposition of tritons in Zone(2); the most pessimistic assumption for tritium retention in the bulk is that the entire tritium source ϕ_T is located at the deepest accessible penetration distance i.e. at $R= R_D+R_T$, and where, under such assumption, the T concentration would be at a maximum (n_T). This situation is depicted schematically in Figure 4. Denoting the diffusive flow of tritium in zones (2) and (3) as ϕ_2 and ϕ_3 respectively:

$$\phi_2 = \frac{D(n_T - n_0)}{R_T} \quad (3)$$

$$\phi_3 = \frac{Dn_T}{L} \quad (4)$$

where D is the thermal diffusion coefficient. In the steady state:

$$\phi_2 + \phi_3 = \phi_T \quad (5)$$

where ϕ_T = $3.78\times10^{9}cm^{-2}s^{-1}$ for a 1MeV incident D beam at $1mAcm^{-2}$ (Section 2.1). The thermal diffusion constant *D* can be estimated as [3]:

$$(6) \qquad D = D_0 \cdot \exp(-\frac{E_D}{kT}) \quad \left[\mathrm{cm}^2 \cdot \mathrm{s}^{-1}\right],$$

where E_D is the energy threshold for the diffusion process (0.4 eV for copper), *k* is the Boltzmann constant ($8.617 \cdot 10^{-5}$ eV/K), *T* the absolute temperature and D_0 = 0.11 $cm^2 \cdot s^{-1}$ for copper. There is however considerable uncertainty in the values of the diffusion coefficient depending on the condition (e.g. degree of ageing) of the material.

During the beam-ON phase the average temperature of the material is assumed to be 200º C, while during the beam-OFF phase the temperature is assumed to be 20º C. Table 3 below summarises the values of the diffusion constant in the two cases.

	Temperature T (K)	**Diffusion Constant *D***
Beam ON	473	$6.04 \cdot 10^{-6}$ $cm^2 \cdot s^{-1}$
Beam OFF	293	$1.46 \cdot 10^{-8}$ $cm^2 \cdot s^{-1}$

Table 3: Hydrogenic thermal diffusion coefficient in Cu at representative temperatures

Equations (3), (4) and (5) may then be solved for ϕ_2, ϕ_3 and n_T using the diffusion coefficient for temperatures representative of the beam-on condition; in the usual approach of maintaining a conservative estimate, it is assumed that the tritium remains "frozen in" during the beam-off periods. The results imply that, after 500 1-hour pulses, $n_T = 1.82\times10^{13}cm^{-3}$ and the ratio ϕ_3 / ϕ_T = 0.17. It may be seen that n_T is only slightly higher than n_0, due to the short distance the bulk tritium has to diffuse in order to reach the D implantation region, Zone(1), from which it is presumed to be effectively "scavenged" by the incoming D beam by isotope exchange. It may be noted that there is much experimental evidence from 'drive-in target' experiments to show that the effective diffusion coefficient in the implantation zone is very much reduced compared with the thermal diffusion coefficient characteristic of undamaged material. This is thought to be due to voids and bubble formation, leading to the high hydrogenic density values needed to explain the levels of neutron production [8]. In zone(2), however, the integrated source of fast tritons is too low to cause significant material damage. The ratio ϕ_3 / ϕ_T = 0.17 implies that most (>80%) of the tritium will be recovered on the beamline cryopump. Most of the remainder will diffuse into the cooling water, and a

proportion will remain “frozen in” after the last pulse. This can be estimated from the integral of the tritium density profile in zone (3), approximately given by $L.n_T/2 = 1.82\times10^{12}cm^{-2}$ i.e. only about 0.03% of the total T production (from Table 2).

4.2 Tritium production/retention for reference campaign

The tritium production is linear with total fluence (Section 2.1) and the discussion of retained fraction is based on 500 1-hour pulses at the maximum D beam current density of $1mAcm^{-2}$. For the reference NBTF programme equivalent to 250 hours of full power beam operation (1MeV, 40A), the total integrated T production is about 0.25TBq. The proportions of tritium retained and released either to the cryopump or cooling water are not strictly constant, because the boundary condition set by n_0, the T density in Zone(1), rises asymptotically with D fluence according to the LMM (Table 1). This implies that in regions of lower power density, where there are lower fluxes and hence lower fluence, the proportion of tritium diffusing to the water and retained in the bulk could be somewhat higher. Conversely, the effect of non-normal beam incidence will reduce the width of zones (1) & (2), measured normal to the surface, thus tending to increase the proportion diffusing towards the surface. However, assuming the proportions as derived in Section 4.1, about 0.2TBq should be collected on the cryopump, 0.05TBq could enter the cooling water circuit and about 70MBq remain “frozen in” to the target material after the last pulse. It may be noted that the latter figure is well within the IAEA exemption limit for a transportation package (1GBq). A prolonged period of operation with hydrogen beams should be effective in removing the tritium from the implantation region (Figure 3). The hydrogen beams will not, however, remove tritium implanted in zones (2) & (3) other than through promoting thermal diffusion by elevating the material temperature. Since the actual tritium production can be accurately measured by measuring the 2.5MeV neutron production from DD reactions, it should be possible to carry out tritium accounting measurements on the vacuum exhaust and cooling water circuit in order to track the tritium and carry out accountancy.

5. **Neutronics and activation**

5.1 Neutron production in the ITER NB Test Facility components

The neutron rate and isotope retention have been calculated for the two highest power receiving ITER NB components, i.e. the Calorimeter and Residual Ion Dump (RID). Other components such as the accelerator grids and the neutraliser also receive power but at a considerably lower level so have not been assessed. The neutronics calculations require a spatial distribution of the neutron source. The approach adopted is described for the NBTF calorimeter (a similar method is used for the RID). The ITER NB Calorimeter is composed of two panels of Swirl Tube Elements (STEs) running horizontally. The two panels are positioned to form a V-shaped structure with an extreme point (vertex) at X=10.4 metres from the ground grid of the source. The calorimeter has been divided into 12 zones longitudinally. Each zone is 0.2 metres long. The power density is considered constant and equal to the vertically averaged value in each zone. The average current density on each zone is plotted in Figure 5 taking into account the vertical power distribution correction mentioned above. The current densities indicated correspond to a total beam current of 15 A per panel or 30 A in the whole calorimeter. This is an over-estimate due to the pessimistic assumptions made in the derivation of the current densities on the component. Table 4 describes the neutron production and isotope retention in the ITER NB Calorimeter after a total working time of 250 hours using the results of Section 2.1 and Table 1.

position	Jbeam	D Fluence	D fluence	DD rate	TD rate
[m]	[mA/cm²]	[C/cm²]	[1/cm²]	neutrons	neutrons
0.100	0.227	204.447	1.276E+21	2.473E+18	3.402E+13
0.300	0.408	367.031	2.291E+21	4.440E+18	6.107E+13
0.500	0.634	570.505	3.561E+21	6.901E+18	9.493E+13
0.700	0.582	523.774	3.270E+21	6.336E+18	8.716E+13
0.900	0.309	278.438	1.738E+21	3.368E+18	4.633E+13
1.100	0.107	96.382	6.016E+20	1.166E+18	1.604E+13
1.300	0.097	87.620	5.469E+20	1.060E+18	1.458E+13
1.500	0.379	340.745	2.127E+21	4.122E+18	5.670E+13
1.700	0.718	646.442	4.035E+21	7.819E+18	1.076E+14
1.900	0.731	658.125	4.108E+21	7.961E+18	1.095E+14
2.100	0.392	352.428	2.200E+21	4.263E+18	5.864E+13
2.300	0.119	107.091	6.685E+20	1.295E+18	1.782E+13

Table 4: Total neutron production on one ITER NB calorimeter panel after 250 hours.

5.2 Representation of NBTF for neutronics calculations

The major components of the injector are the high voltage (HV) bushing, the beam source, the neutraliser, the residual ion dump, the calorimeter and the cryopump. These are all

contained in a single vacuum vessel. Each of these components was included in the MCNP model (Figure 6). However some approximations were made since all the details are not required and the creation of the model is very time consuming. The elemental weight distribution corresponding to the different materials was entered into cells making up the representation of each component. The beam is deposited equally on each calorimeter panel and the deposition on each RID panel is constant but the deposition along the lengths of the calorimeter and RID panels is not uniform and so the neutron production is distributed in a complex manner across these components, using input data similar to Table 4. This non-uniformity was reproduced in the source representation in MCNP. The Monte-Carlo code MCNP was used to determine the energy dependent neutron flux in all material cells. These results were then used in the subsequent activation calculations. MCNP was also used to estimate the neutron dose during beam operation at a location outside the test cell shielding, assumed to be made of boronated concrete.

5.3 Activation calculations

To compute the activation of the components, the energy dependent neutron flux and the irradiation history must be specified. The neutron spectra were available in Vitamin J energy group structure from the MCNP calculations described above. The irradiation, or neutron production history was based on the reference programme i.e. 300 days with 100 pulses per day with each pulse lasting 20 seconds. This is followed by 14 days of a full power programme with 6 one hour pulses per day. Only the pulses in the full power programme were explicitly described in the activation calculations. The 300 day programme was described as a continuous irradiation at a level which conserved the total neutron production. The activation calculations were carried out using the inventory code FISPACT. This provided the activity, and contact dose rates for all components after cooling times of 1, 5, 10, 30, 60, 120 and 365 days. It also provided 24 energy group descriptions of the gamma-ray spectra emitted from each cell. These were used as input to gamma dose calculations.

5.4 Brief summary of activation results for NBTF

It is convenient to consider the activation of the components by categorising them according to the material of which they are made, namely, stainless steel, copper CuCrZr and

alumina. Homogenised mixtures of water and these materials were used for some components in the neutron transport modelling but the coolant was removed for the activation calculations. It was established from the LMM code that the DT yield is substantially less than the DD yield and the predicted activation by 14MeV neutrons is four orders of magnitude lower; within the time-scale of up to one year, activation by 14MeV neutrons is insignificant despite the fact that the higher energy permits access to more threshold reactions. The components which are most strongly activated (by 2.5MeV neutrons) are the cooling pipes and mountings of the calorimeter and the RID. Only seven components have activities above the IAEA limit of 7×10^{4} Bq/kg (i.e. they would be classified as low level waste (LLW)) after one year although several are initially classified as LLW at earlier times. The lower cooling manifold of the calorimeter, and RID and calorimeter support structures would however also give a contact dose in excess of 10^{-5} Sv/hr (the "hands on" limit) after 1 year.

6. **Conclusions**

The Local Mixing Model, has been adapted in order to model both 2.5 and 14MeV neutron production in deuterium beam-target reactions, together with the tritium production rate. The tritium, produced by DD reactions, is treated as part of the incoming deuterium beam but this approach has a number of limitations which have been discussed in detail. In particular, the 'birth' position, the angular and the energy distributions of the tritons are not taken into account in the code. This means that the tritons can travel deeper into the target material than the LMM code predicts. The consequences of this are that the prediction of the 14MeV neutron rate is pessimistic and the prediction of the tritium retention in the material is optimistic. However, the LMM may be combined with a thermal diffusion model for the retained tritium that leads to more realistic predictions of tritium retention that should still maintain a conservative margin. The neutron source rates have been used as input into neutronics and activation calculations for the NBTF based on a reference programme describing its operational lifetime. The individual components of the injector are found generally not to be activated excessively, and with the exception of three localised stainless steel components located closest to the most intense neutron sources, the majority of components' activation levels fall below the hands on limit within one year.

References

[1] D K Brice, Steady State Hydrogen Transport in Solids Exposed to Fusion Reactor Plasmas, J Nucl Mat 120 (1984) 230-244

[2] H-D Falter *et al*, 17th Symposium on Fusion Technology, Rome (1992) p 481

[3] H-D Falter, Gas Absorption, Re-Emission and Permeation in Beam Stopping Panels, JET-DN-C(88)57 (JET Joint Undertaking internal report)

[4] J F Briesmeister, editor, MCNP™ - a General Monte Carlo N-Particle Transport Code" Los Alamos National Laboratory Report, LA-13709-M (March 2000), version 4C3

[5] R Forrest "FISPACT 2003: User Manual" UKAEA Fusion, UKAEA Internal Report, FUS 485 (December 2002) http://www.fusion.org.uk/techdocs/ukaea-fus-485.pdf

[6] M Fumelli *et al*, Powerful 160 keV neutral deuterium beam injector for application in research, Rev Sci Instr, 57(7) (1985) p 1266

[7] J Kim, D-D Neutron and X-ray Yields from High-Power Deuterium Beam Injectors, Nucl Tech 44 (1979) p 315

[8] J Kim, Neutron Sources Using D-T Mixed Beams Driven into Solid Target, Nucl Instr and Meth (1977) 145, p 9

[9] ITER Design Description Document (DDD 5.3) Neutral Beam Heating & Current Drive (NB H&CD) System (ITER Report N 53 DDD 29 01-07-03 R 0.1)

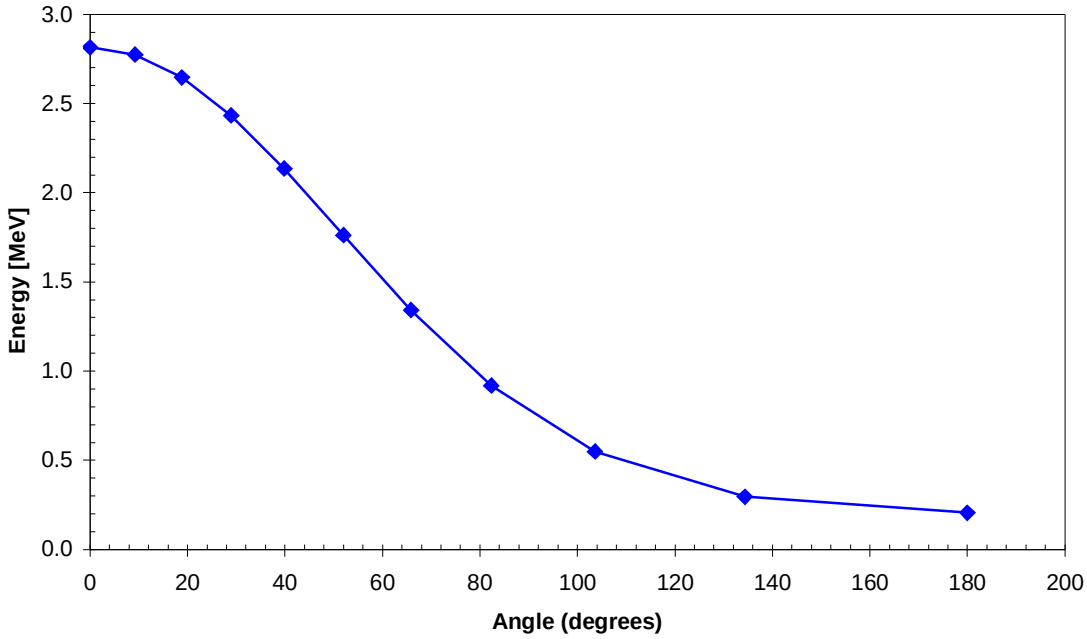

Figure 1: Angular distribution of the energy of the T generated in the DD reaction. The angle is the angle between the incoming D and the generated T

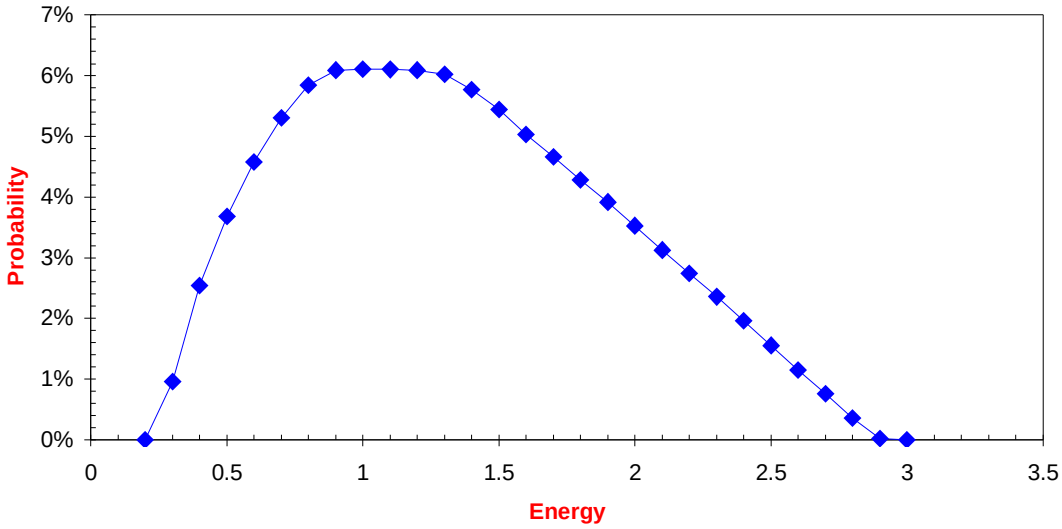

Figure 2: Probability distribution of the energy of the T generated from the fusion of a 1 MeV D projectile and a D target

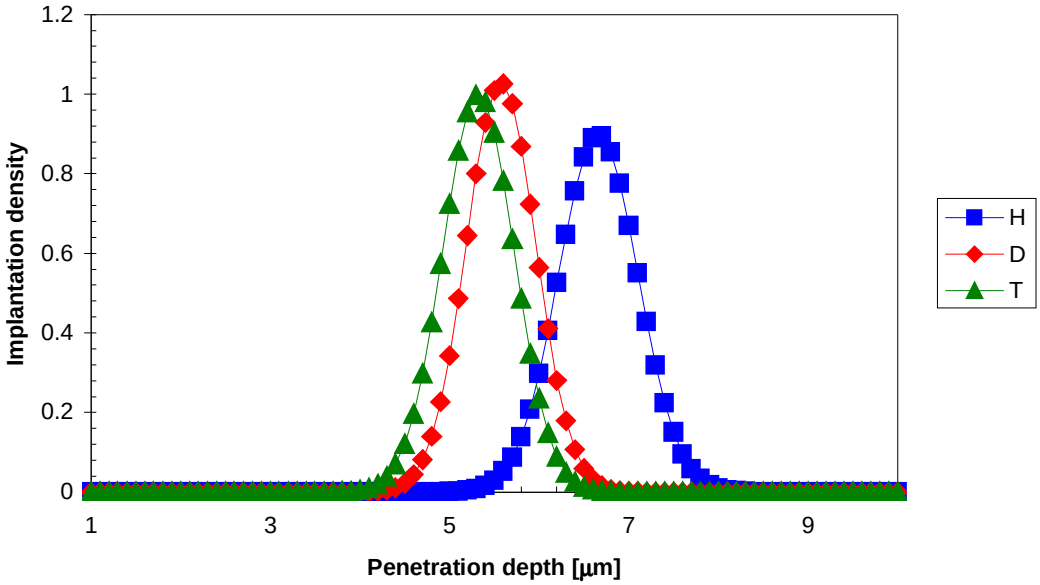

Figure 3: Implantation distribution of the three isotopes for a beam of 1MeV energy on copper

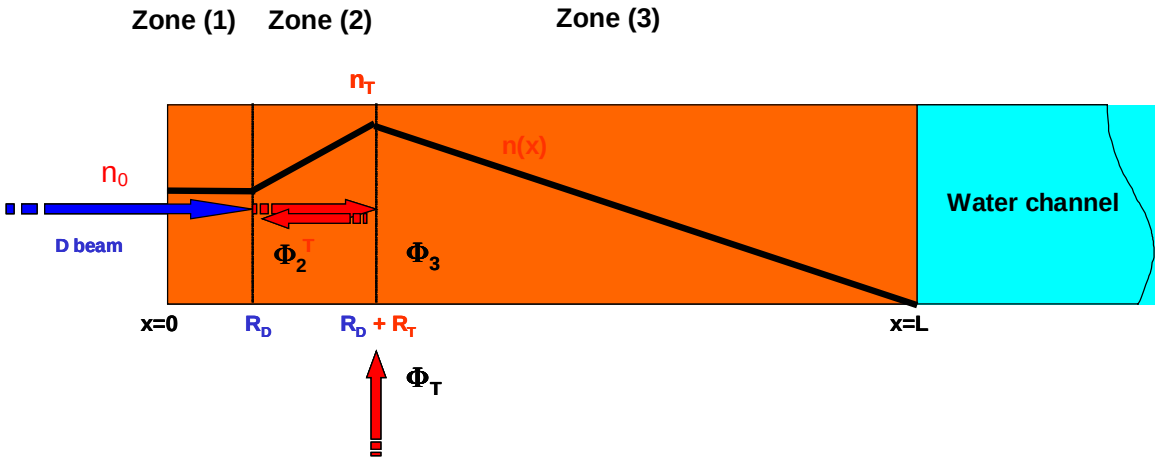

Figure 4: Schematic diagram of implantation and thermal diffusion zones

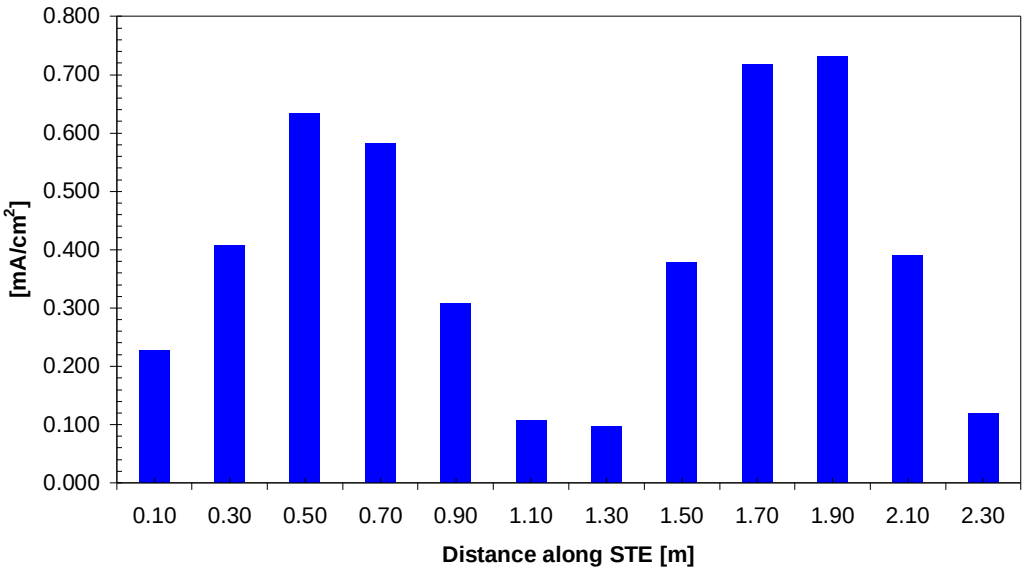

Figure 5: Average beam current density in each zone of one ITER NB Calorimeter panel

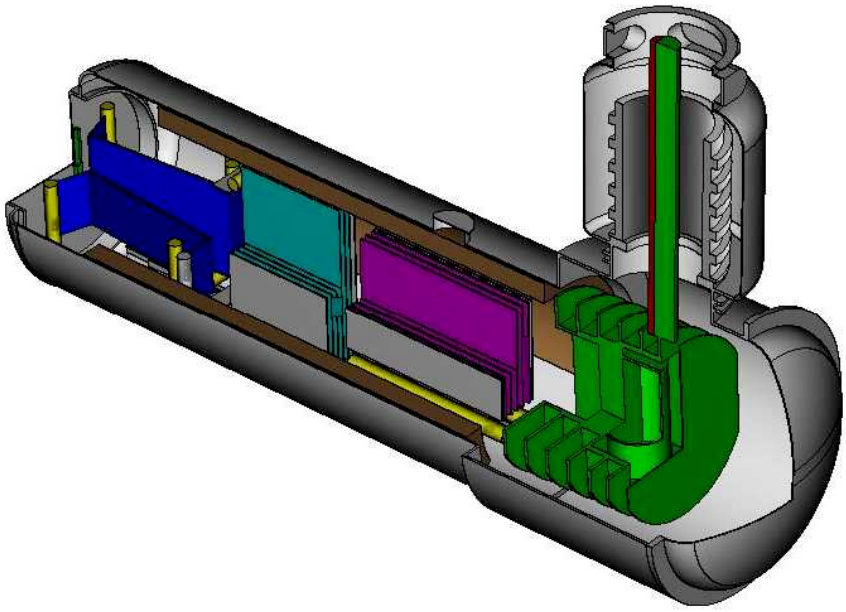

Figure 6: Cutaway iso view of MCNP model of neutral beam injector showing (from top right to bottom left) main NBTF components: HV bushing, beam source, neutraliser, Residual Ion Dump and Calorimeter